The final publication is available at

http://doi.org/10.1007/s11244-018-1043-x

Additional Information

Graphene film-supported oriented 1.1.1 gold (0) versus 2.0.0 copper (I) nanoplatelets as very efficient catalysts for coupling reactions

Natalia Candu,[a] Andrada Simion,[a] Simona M. Coman,[a] Ana Primo,[b] Ivan Esteve-Adell,[b] Vasile I. Parvulescu,[a*] Hermenegildo Garcia[b*]

[a] *Department of Organic Chemistry, Biochemistry and Catalysis, University of Bucharest, Bd. Regina Elisabeta no. 4–12, 030018 Bucharest 030016, Romania*

[b] *Instituto Universitario de Tecnologia Quimica Consejo Superior de Investigaciones Científicas-Universitat Politecnica de Valencia, Universidad Politecnica de Valencia, Avda. de los Naranjos s/n, Valencia 46022, Spain*

Abstract: Few-layered graphene-supported 1.1.1 and 2.0.0 oriented Au and Cu_2O nanoplatelets were prepared by one-step pyrolysis of the corresponding metal salts embedded in chitosan at 900 °C under inert atmosphere. These nanometric films containing oriented nanoplatelets were investigated in a series of reactions as Ullmann-type homocoupling, C–N cross-coupling and Michael addition. The catalysts exhibited turnover numbers (TONs) three to six orders of magnitude higher than those of analogous graphene-supported unoriented metal nanoparticles. In addition it has been found that oriented Cu_2O and Au nanoplatelets grafted on defective graphene also exhibit activity to promote the Michael addition of compounds with active methylene and methine hydrogens to α,β−conjugated ketone. An exhaustive characterization of these materials using spectroscopic and electron microscopy analyses has been carried out. CO_2 thermoprogrammed desorption measurements show that films of these two graphene supported catalysts exhibit some basicity that can explain their activity to promote Michael addition.

Corresponding authors: vasile.parvulescu@chimie.unibuc.ro; hgarcia@qim.upv.es

1. Introduction

Metal nanoparticles (MNPs) supported on high surface area solids represent a large field of investigation and have become among the best heterogeneous catalysts for a large variety of organic reactions [F. Tao (Editor), Metal Nanoparticles for Catalysis : Advances and Applications, RSC

Catalysis Series, RSC, 2016]. In this area, development of new protocols for the synthesis of MNPs having tuned electronic properties by interaction with the support and/or exposing preferential facets are among the most important targets in order to achieve an optimal catalytic performance. In this context, the existing literature already suggests that carbon-nanotubes [G.G. Wildgoose, C.E. Banks, R.G. Compton, *Small* **2006**, *2*, 182–193] and, more recently, graphene [M. Ding, Y. Tang, A. Star, *J. Phys. Chem. Lett*. **2013**, *4*, 147–160] provide interfaces with MNPs exhibiting specific electronic properties due to the occurrence of charge transfer between the carbon nanoform and the MNPs.

In this context, we have recently shown a novel procedure for the preparation in one-step pyrolysis of MNPs strongly grafted on few- and multilayer defective graphenes by pyrolysis of natural polysaccharides containing metal salts [Primo, A., Esteve, I., Blandez, J. f., Dhakshinamoorthy, A., Alvaro, M., Candu, N., Coman, S., Parvulescu, V.I., Garcia, H. *Nature Commun*., (2015), *Article number: 8561*]. Chitosan has the ability to adsorb metal ions in aqueous solutions by strong interactions of the positive amino groups of the glucosamine units of the polymer fibrils with metal ions, *e.g.* $AuCl_4^-$ and Cu^{2+}, among others. In fact, chitosan and related natural polysaccharides are already widely used in water purification treatments as trapping agents of undesirable metal ions present in aqueous solution, e.g. Cu^{2+} [Ravi Kumar, M. N. V., React. Funct. Polym. 46 (2000) 1–27; Rinaudo, M., Prog. Polym. Sci. 31 (2006) 603–632; Rinaudo, M., Polym. Int. 57 (2008) 397–430]. In these reports, it was found that pyrolysis of thin films of chitosan and other filmogenic natural biopolymers can provide *fl*-G (*fl* meaning few layers structures; G meaning defective graphene) of few nanometers thickness [Primo, A., Atienzar, P., Sanchez, E., Delgado, J. M. and Garcia, H., Chem. Commun. 48 (2012) 9254–9256; Primo, A., Sa´nchez, E., Delgado, J. M. and Garcia, H., Carbon 68 (2014) 777–783; Primo, A., Forneli, A., Corma, A. and Garcia, H. ChemSusChem 5 (2012) 2207–2214]. In the pyrolysis process, chitosan films containing $AuCl_4^-$ or Cu^{2+} ions renders 1.1.1 facet oriented Au and Cu nanoplatelets strongly grafted on defective N-doped graphene film, the number of layers depending on the thickness of the chitosan film precursor. This material arises as consequence of the strong reductive conditions of the G synthesis and the low solubility of Au and Cu in carbon that makes them segregate as an independent phase [X. Li, W. Cai, J. An, S. Kim, J. Nah, D. Yang, R. Piner, A. Velamakanni, I. Jung, E. Tutuc, S. K. Banerjee, L. Colombo, R. S. Ruoff, Science, 2009, 324, 1312 – 1314; D. Takagi, Y. Kobayashi, H. Hlbirio, S. Suzuki, Y. Homma, Nano Lett., 2008, 8, 832 – 835]. In spite of the high pyrolysis temperature, the resulting MNPs exhibit a relatively moderate size in the range of 10-20 nm, presumably because the carbonaceous residues present at each stage of the pyrolysis arrest the growth of the insoluble Au or Cu NPs.

To rationalize the preferential facet exposed by the MNPs on top of *fl*-G films, a reverse templating mechanism inspired in the preparation procedure of high electronic quality G films by

chemical vapor deposition (CVD) was proposed [Reina, A. et al. Nano Lett. 9, 30–35 (2008); Wei, D. et al.. Nano Lett. 9, 1752–1758 (2009); Kim, K. S. et al. Nature 457, 706–710 (2009)]. In CVD, experimental evidence has proved that the 1.1.1 facet of Cu films is more suited to form high-quality G compared to the 1.0.0 facet that matches worse with the symmetry and dimensions of G [Gao, L., Guest, J. R. & Guisinguer, N. P., Nano Lett. 10, 3512–3516 (2010); Zhao, L. et al., Solid State Commun. 151, 509–513 (2011); Wood, J. D., Schmucker, S. W., Lyons, A. S., Pop, E., Lyding, J. W., Nano Lett. 11, 4547–4554 (2011)]. The suggested hypothesis was that the same principles should also apply for the reverse process, where the G sheets developing in the pyrolysis process earlier than the MNPs could drive the growth of them into a preferential crystallographic plane.

Indeed, pyrolysis at 900 °C under inert atmosphere of copper(II) nitrate embedded in chitosan films afforded 1.1.1 facet-oriented copper nanoplatelets supported on few-layered graphene ($\overline{Cu}$/fl-G, $\overline{Cu}$ meaning 1.1.1 oriented Cu NPs) [Primo, A., Esteve, I., Blandez, J. F., Dhakshinamoorthy, A., Alvaro, M., Candu, N., Coman, S., Parvulescu, V., Garcia, H. *Nature Commun*., (2015), *Article number: 8561*]. $\overline{Cu}$/fl-G undergoes upon exposure to the ambient for a few hours a spontaneous oxidation to render preferentially oriented (2.0.0) copper(I) oxide nanoplatelets on few-layer graphene ($\overline{Cu_2O}$/fl-G). Similarly, the pyrolysis of chitosan films containing Au^{3+} render 1.1.1 oriented Au nanoplatelets (20 nm lateral size, 3–4 nm height) on a few layers of N-doped graphene ($\overline{Au}$/fl-G), while the lateral sides also correspond to 0.0.1 oriented planes [Primo A., Esteve-Adell I., Candu N., Coman S., Parvulescu V., Garcia H., *Angew. Chem.-Int. Ed.,* 55 (2) (2016) 607-612].

Comparison of the catalytic activity of $\overline{Au}$/fl-G films with powders of unoriented Au NPs supported on graphene showed that $\overline{Au}$/fl-G films exhibit almost six orders of magnitude enhancement of catalytic activity in three different Au catalyzed reactions, namely, Ullmann-like homocoupling, C-N cross coupling, and the oxidative coupling of benzene to benzoic acid [Primo A., Esteve-Adell I., Candu N., Coman S., Parvulescu V., Garcia H., *Angew. Chem.-Int. Ed.,* 55 (2016) 607-612]. Similarly, the use of $\overline{Cu_2O}$/fl-G films as catalysts in other three typical Cu(I) catalyzed couplings (*ie,* the Ullmann-like reaction, dehydrogenative silane coupling with alcohols and the Buchwald crosscoupling) showed an increase of about four orders of the intrinsic activity of the 2.0.0 oriented Cu_2O nanoplatelets strongly grafted on G compared to analogous samples of Cu_2O NPs deposited on preformed *fl*-G catalyst [Primo, A., Esteve, I., Blandez, J. F., Dhakshinamoorthy, A., Alvaro, M., Candu, N., Coman, S., Parvulescu, V., Garcia, H. *Nature Commun*., (2015), *Article number: 8561*].

In view of these precedents, it is of interest to expand further the study of the catalytic activity of facet oriented MNP grafted on defective G films as catalysts for different reaction types. In this regard, the Michael addition of active methylene (and methine) compounds to conjugated π-systems is one of the oldest and more useful C-C bond-forming reactions [Jung, M.E. "Stabilized Nucleophiles with Electron Deficient Alkenes and Alkynes". In *Comprehensive Organic Synthesis*; Trost, B. M.;

Fleming, I.; Eds; Pergamon Press: Elmsford, NY, 1991; Vol. 4, Ch. 1.1; Perlmutter, P. *Conjugate Addition Reactions in Organic Synthesis*; Pergamon Press: Elmsford, NY, 1992]. This 1,4-addition is typically carried out using basic catalysts. However, the required basic catalysis may generate by-products arising from competing side reactions. To expand the scope of Michael addition avoiding the use of bases, catalysis by transition metals (*ie*, iron, ruthenium, cobalt, rhodium, iridium, nickel, palladium, platinum, copper and silver) or lanthanides (*ie*, scandium, lanthanum, cerium, samarium, europium, and ytterbium) under neutral conditions has attracted the attention of the chemical community [for review see: Christoffers, J. Eur. J. Org. Chem. 1998, 1259–1266; Comelles, J.;Moreno-Mañas, M.; Vallribera, A. Arkivoc 2005, (part ix), 207–238]. Following the pioneering work by Saegusa's group, among these metals, Cu is among the metals that has attracted larger attention as catalyst for these Michael additions [Saegusa, T.; Ito, Y.; Tomitra, S.; Kinoshita, H. *Bull. Chem. Soc. Jpn*. **1972**, *45*, 496]. Improvements of the reaction performance have been reported under microwave irradiation which accelerates the Michael addition of diketones, ketoesters, and malonates to methyl vinyl ketone (MVK) in the presence of various metal acetylacetonates (as Cr(III), Mn(II), Fe(III), Co(II), Ni(II), or Cu(II)) as catalysts [Hidehiko, K.; Masahiro, S.; Nagata, C. *Nippon Kagaku Kaishi* **1999**, 145; *Chem. Abstr*. 130:267140].

More recently, Mattoussi et al.[Oh, E.; Susumu, K.; Blanco-Canosa, J. B.; Medintz, I. L.; Dawson, P. E.; Mattoussi, H. Small 2010, 12, 1273] and Rodriguez-Fernández et al [Ba, H.; Rodriguez-Fernández, J.; Stefani, F. D.; Feldman, J. Nano Lett. 2010, 10, 3006] have demonstrated the efficiency of water soluble, large (>15 nm) maleimide modified Au NPs as Michael catalysts for bioconjugation applications. Later, maleimide functionalized Au (I) NPs was further modified through Michael addition and used as catalyst for Diels-Alder and 1,3 dipolar cycloadditions [K. D. Hartlen, H. Ismaili, J. Zhu, M. S. Workentin, Langmuir 2012, 28, 864–871]. The possibility to use this Michael addition strategy for small sized Au NPs in protic solvents is limited by their solubility. Therefore, application of Au NPs as general catalysts for the Michael additions encounters still some problems related to poor performance and stability.

Following the exploitation of the unique properties of $\overline{Cu_2O}$/*fl-G* and $\overline{Au}$/*fl-G* as catalysts, this article reports that these two graphene grafted MNPs successfully catalyze the Michael addition.

2. Results and discussion

The preparation and characterization of $\overline{Cu_2O}$/*fl-G* and $\overline{Au}$/*fl-G* materials has been reported in detail in our previous works [Primo, A., Esteve, I., Blandez, J. F., Dhakshinamoorthy, A., Alvaro, M., Candu, N., Coman, S., Parvulescu, V., Garcia, H. *Nature Commun*., (2015), *Article number:*

8561; Primo A., Esteve-Adell I., Candu N., Coman S., Parvulescu V., Garcia H., *Angew. Chem.-Int. Ed.,* 55 (2) (2016) 607-612]. Briefly, it was found that the oriented $\overline{Cu/fl}$-G films are constituted by 3 nm height Cu nanoplatelets with preferential 1.1.1 facets [Primo, A., Esteve, I., Blandez, J. F., Dhakshinamoorthy, A., Alvaro, M., Candu, N., Coman, S., Parvulescu, V., Garcia, H. *Nature Commun.,* (2015), *Article number: 8561*], presumably as result of the epitaxial templation by G of the nascent Cu nanoplatelets during phase segregation at temperatures higher than 800 °C. Further, the spontaneous oxidation of $\overline{Cu/fl}$-G affords oriented $\overline{Cu_2O/fl}$-G constituted by Cu_2O nanoplatelets with about 82 % of the particles exhibiting a preferential 2.0.0 facet orientation, as determined by Raman spectroscopy and TEM images combined with analysis of the diffraction pattern of back scattered electrons. In the case of $\overline{Au/fl}$-G sample, TEM images and Raman spectrum revealed that the preferential morphology of Au nanocrystals is nanoplatelets, whose size distribution and average dimensions depend on the concentration of Au on chitosan. However, 1.1.1 facet orientation was preferentially formed, regardless of the Au loading and the thickness of G [Primo A., Esteve-Adell I., Candu N., Coman S., Parvulescu V., Garcia H., *Angew. Chem.-Int. Ed.,* 55 (2) (2016) 607-612].

The subnanometric vertical resolution of the AFM analysis [Primo, A., Esteve, I., Blandez, J. F., Dhakshinamoorthy, A., Alvaro, M., Candu, N., Coman, S., Parvulescu, V., Garcia, H. *Nature Commun.,* (2015), *Article number: 8561*; Primo A., Esteve-Adell I., Candu N., Coman S., Parvulescu V., Garcia H., *Angew. Chem.-Int. Ed.,* 55 (2) (2016) 607-612] showed that both Cu and Au nanoplatelets have an average high of about 3 nm and the frontal views showed that these thin metal nanoplatelets are homogenously distributed on top of the *fl*-G film (Figure 1a). FESEM images suggest a high crystallinity and ordering of the metal atoms (Figure 1 b, c).
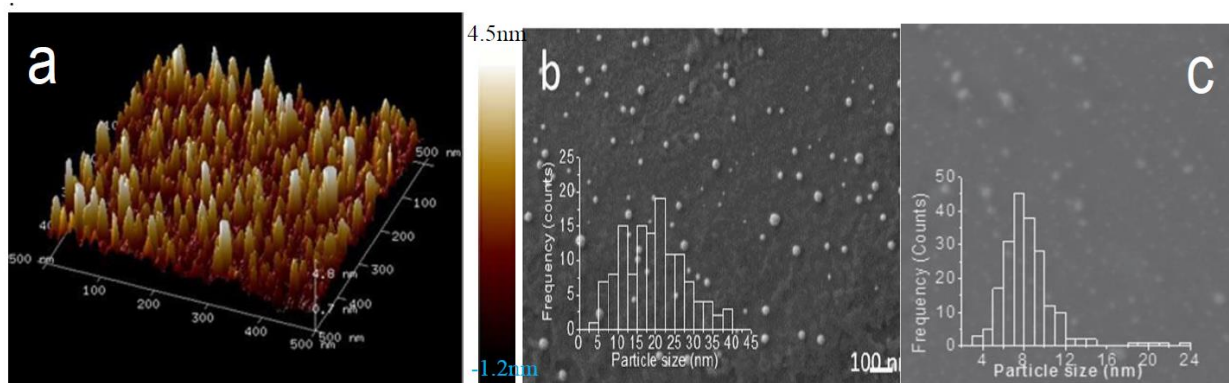
Figure 1. Three-dimensional AFM image of $\overline{Cu/fl}$-G (0.5 × 0.5 μm) (**a**); FESEM images of oriented $\overline{Au/fl}$-G (**b**) and $\overline{Cu/fl}$-G (**c**) on few or multi layers G [Primo, A., Esteve, I., Blandez, J. F., Dhakshinamoorthy, A., Alvaro, M., Candu, N., Coman, S., Parvulescu, V., Garcia, H. *Nature Commun.,* (2015), *Article number: 8561*; Primo A., Esteve-Adell I., Candu N., Coman S., Parvulescu V., Garcia H., *Angew. Chem.-Int. Ed.,* 55 (2) (2016) 607-612].

XRD and XPS techniques were also in agreement with the above statements. Owing to the low film thickness and metal loading, XRD analysis of $\overline{\overline{Au}}$/fl-G and $\overline{\overline{Cu}}$/fl-G samples did not exhibit any diffraction lines. However, thicker $\overline{\overline{Au}}$/ml-G samples of multilayer G (thickness > 40 nm, *ml* standing for multilayer) exhibited a single peak at 39°, attributed to the 1.1.1 facet orientation accompanied by a weaker 2.2.2 peak at 82° (Figure 2a). In the same way, the XRD of the pyrolyzed Cu^{2+}-chitosan films (*ie*, corresponding to $\overline{\overline{Cu}}$/ml-G sample) exhibits almost exclusively a single diffraction line corresponding to the 1.1.1 plane (Figure 2b) constituting a firm evidence that Cu NPs present immediately after pyrolysis exhibit oriented facets when grown following the pyrolysis method of chitosan films.
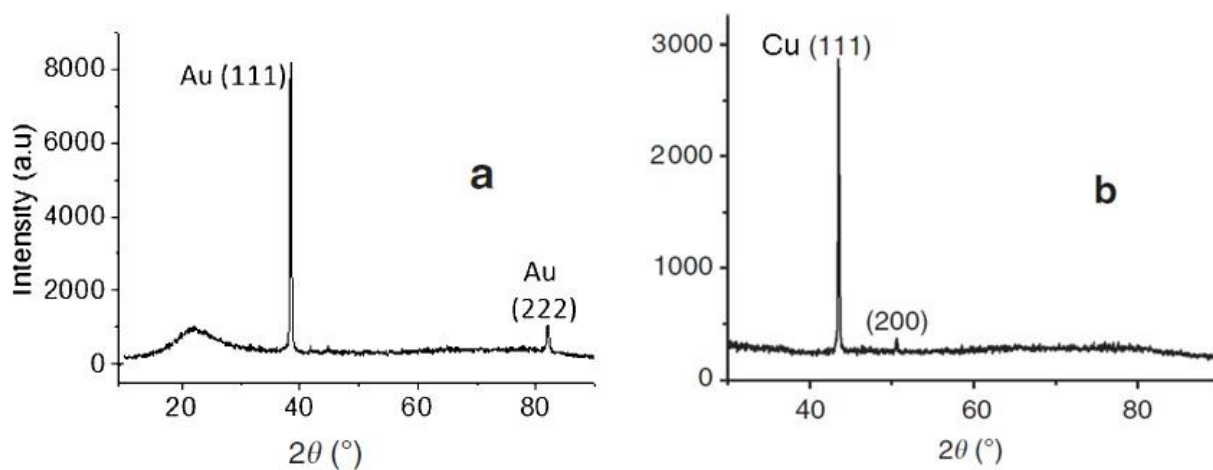
Figure 2. XRD patterns of $\overline{\overline{Au}}$/ml-G (**a**) and $\overline{\overline{Cu}}$/ml-G (**b**) samples. The broad diffraction line at about 22° (**a**) corresponds to characteristic diffraction of *ml-G* [Primo, A., Esteve, I., Blandez, J. F., Dhakshinamoorthy, A., Alvaro, M., Candu, N., Coman, S., Parvulescu, V., Garcia, H. *Nature Commun.*, (2015), *Article number: 8561*; Primo A., Esteve-Adell I., Candu N., Coman S., Parvulescu V., Garcia H., *Angew. Chem.-Int. Ed.,* 55 (2) (2016) 607-612].

Upon storage, $\overline{\overline{Cu}}$/fl-G films convert to $\overline{\overline{Cu_2}}$O/fl-G films as determined by Raman and XP spectroscopies. In XPS, analysis of the high-resolution Cu2p peak shows the presence of Cu(I) and Cu(II) on the outermost layers of oriented $\overline{\overline{Cu_2}}$O/fl-G films (Figure 3a). In contrast, the shape of the experimental Au 4f peak indicated the presence of a single component, Au(0), without significant contribution of Au(I) and Au(III) in $\overline{\overline{Au}}$/fl-G film (Figure 3b).
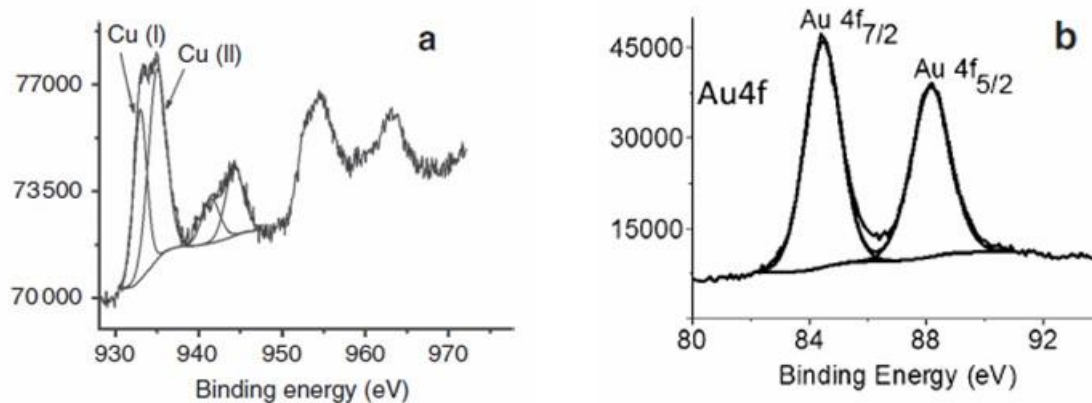
Figure 3. XPS Cu 2p (**a**) and Au 4f (**b**) peaks, as well as their best fitting to individual components recorded for the $\overline{Cu/fl}$-G (**a**) and $\overline{Au/fl}$-G (**b**) samples [Primo, A., Esteve, I., Blandez, J. F., Dhakshinamoorthy, A., Alvaro, M., Candu, N., Coman, S., Parvulescu, V., Garcia, H. *Nature Commun.*, (2015), *Article number: 8561*; Primo A., Esteve-Adell I., Candu N., Coman S., Parvulescu V., Garcia H., *Angew. Chem.-Int. Ed.*, 55 (2) (2016) 607-612]

These films containing oriented Cu_2O and oriented Au(0) exhibit as catalysts exhibit TON values that can be from three to even six orders of magnitude higher for the Ullmann-type homocoupling (Scheme 1 and Figure 4A) and C–N cross-coupling (Scheme 1 and Figure 4B) than those of analogous unoriented graphene-supported Cu_2O NPs.
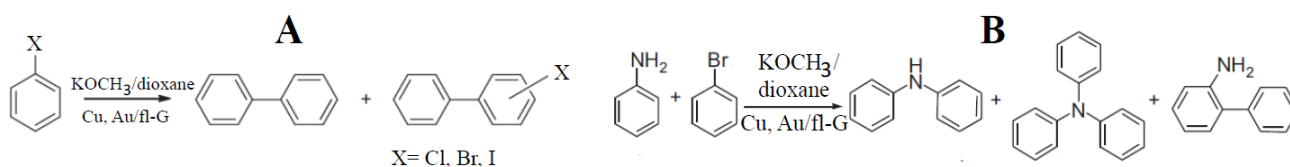
Scheme 1. Products observed in the Ullmann-type homocoupling (**A**) and C–N cross-coupling (**B**) of aniline and bromobenzene catalyzed by oriented and unoriented Cu_2O and Au NPs supported on defective G.
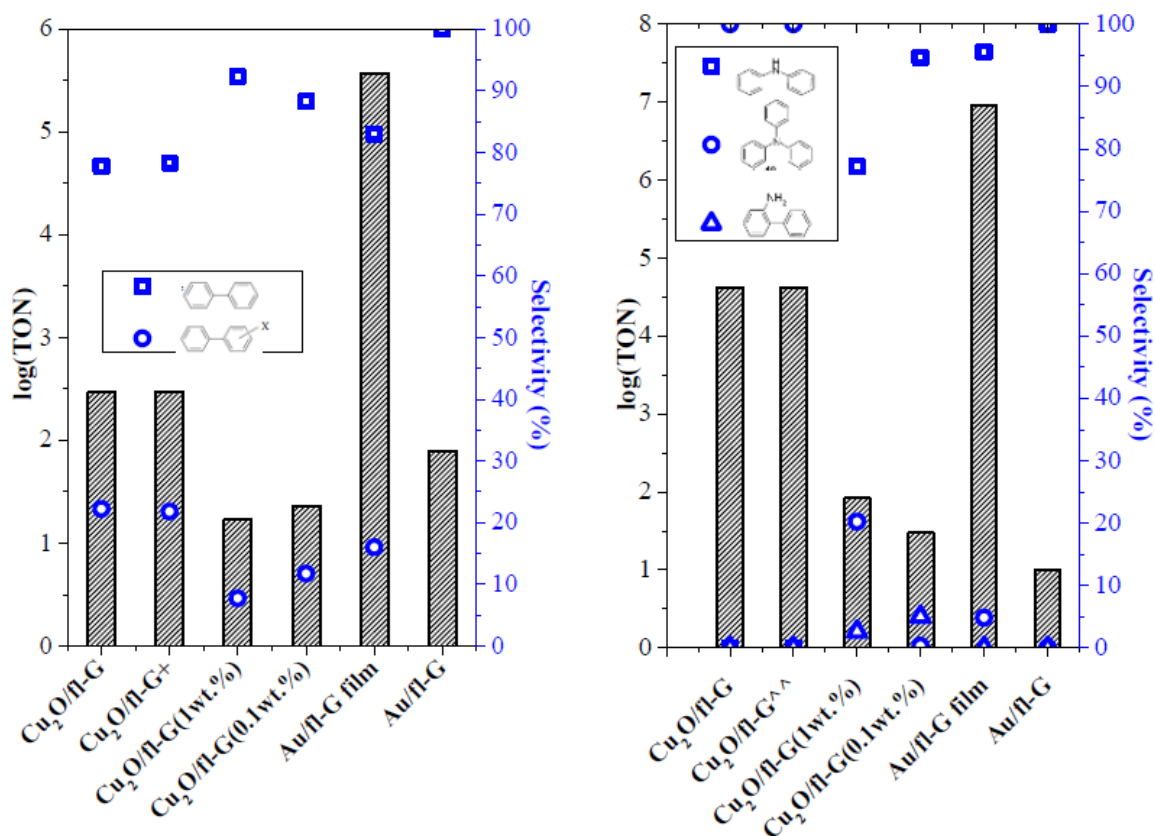
Figure 4. Catalytic results in Ullmann-type homocoupling (**A**) and C-N cross-coupling (**B**) reactions

It was proposed that these higher catalytic activity of films of oriented metal and metal oxide NPs on graphene is a reflection of the combination of a strong metal–support interaction and preferential facet orientation exposed by the nanoplatelets. On the other hand, as Figures 4A and 4B shows, irrespective of the reaction type (*ie*, Ullmann-type homocoupling (A) and C-N cross-coupling (B)), $\overline{Au}$/fl-G catalyst displays a higher TON than the corresponding $\overline{Cu_2O}$/fl-G material.

Very important too, for the Ullmann-like homocoupling, the selectivity to the reaction products (ie, diphenyl and (*o and p*)-halogeno-diphenyl) has the same trend (ie, higher selectivities to diphenyl in detriment of (*o* and *p*)-halogeno-diphenyl), irrespective of the catalyst nature (ie, $\overline{Cu_2O}$/fl-G or $\overline{Au}$/fl-G). For the C-N coupling the main product in the presence of $\overline{Cu_2O}$/fl-G was triphenylamine, while $\overline{Au}$/fl-G favored the selective formation of diphenylamine [Primo, A., Esteve, I., Blandez, J. F., Dhakshinamoorthy, A., Alvaro, M., Candu, N., Coman, S., Parvulescu, V., Garcia, H. *Nature Commun.*, (2015), *Article number: 8561*; Primo A., Esteve-Adell I., Candu N., Coman S., Parvulescu V., Garcia H., *Angew. Chem.-Int. Ed.,* 55 (2) (2016) 607-612].

Besides coupling reactions, the catalytic performance of oriented nanoplatelets on graphene was also tested for a reaction type with completely different mechanism. The results in the Michael addition of a series of activated methylene substrates as methyl acetoacetate (MeAcOAc), ethyl

8

acetoacetate (EtAcOAc), isobutyl acetoacetate (IsoBuAcOAc) (Scheme 2) as well as of two cyclic esters, *ie*, ethyl 2-oxocyclohexane carboxylate (EtOCH) and ethyl 2-oxocyclopentane carboxylate (EtOCP) (Scheme 3) with methyl vinyl ketone (MVK) in the presence of $\overline{Cu_2O/fl}$-G or $\overline{Au/fl}$-G catalysts are listed in Tables 1 and 2.

R=CH₃, C₂H₅, C₄H₉ (isobutyl)

Michael adduct 1 (1.4)   Michael adduct 2
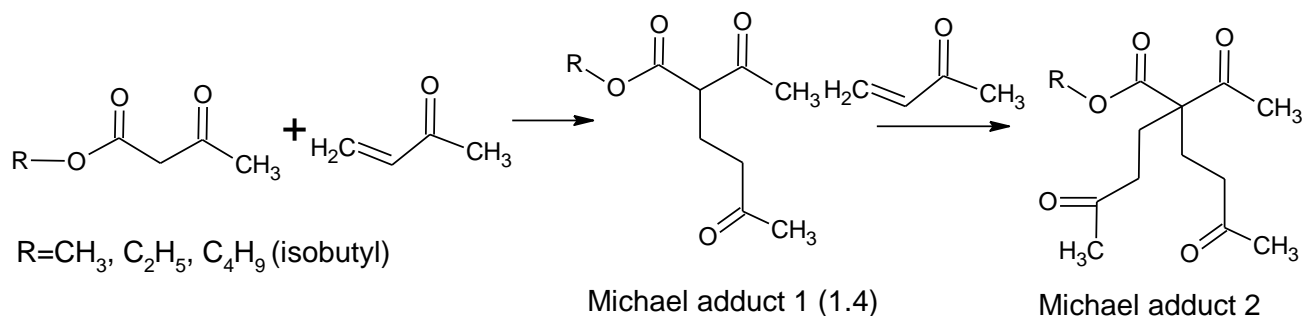
Scheme 2. Michael addition of acetoacetates with MVK

Table 1. Catalytic efficiency of $\overline{Cu_2O/fl}$-G or $\overline{Au/fl}$-G films as catalysts in Michael addition of acetoacetates donors with MVK acceptor

Entry	Michael donor	Base	Catalyst	Conversion (%)	Selectivity (%) MA1	Selectivity (%) MA 2
			$\overline{Au/fl}$-G			
1	MeAcOAc	NaOH	no	84.9	28.8	71.2
2	MeAcOAc	-	yes	44.4	94.5	5.5
3[a]	MeAcOAc	-	yes	28.9	77.1	22.9
4	EtAcOAc	-	yes	97.0	45.7	39.6
5	IsButAcOAc	-	yes	90.8	66.5	33.5
			$\overline{Cu_2O/fl}$-G			
6	MeAcOAc	-	yes	40.1	97.4	2.6
7	EtAcOAc	-	yes	92.3	63.1	36.9
8	IsButAcOAc	-	yes	87.5	71.2	28.8

Reaction conditions: Michael donor: 1 mmol, Michael acceptor: 1.5 mmol, 0.12 mmoles NaOH or absent, 8 ml H₂O, time: 18 h, temperature: RT; or ᵃ50 ºC; Note: Conversion refers to Michael donor transformation.
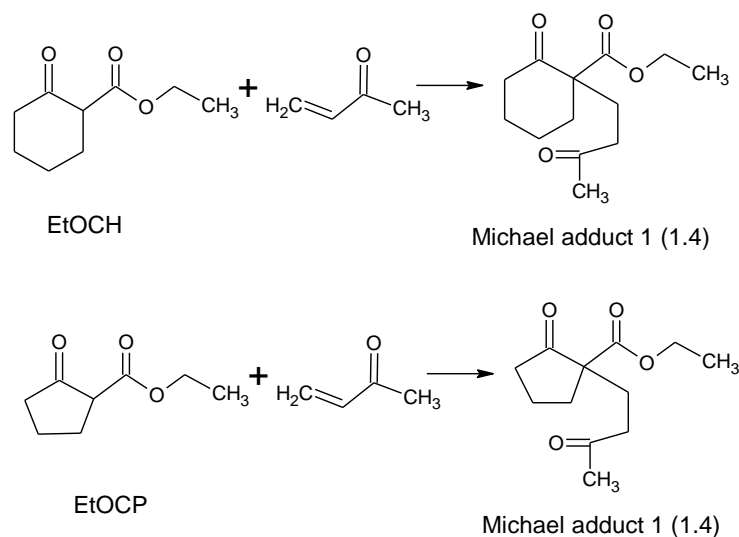
Scheme 2. Michael addition of cyclic esters (Michael donor) with MVK (Michael acceptor)

Table 2. Catalytic efficiency of $\overline{Cu_2O}$/fl-G and $\overline{Au}$/fl-G catalysts in the Michael addition of cyclic esters donors with MVK acceptor

Entry	Michael donor	Conversion (%)	Selectivity (%) MA1
		$\overline{Au}$/fl-G	
1	EtOCH	42.0	100
2	EtOCP	47.6	100
		$\overline{Cu_2O}$/fl-G	
3	EtOCH	40.3	100
4	EtOCP	52.1	100

Reaction conditions: Michael donor: 1 mmol, Michael acceptor: 1,5 mmol (MVK), 8 ml H$_2$O, 18 h, room temperature. Note: Conversion refers to Michael donor transformation.

Using acetoacetates as Michael donors (Scheme 1 and Table 1), the reaction may proceed in two steps. Thus, the remaining active methylene hydrogen in the mono adduct MA1 product can be subsequently deprotonated, resulting in the addition of another MVK molecule with the formation of the MA2 product. Obviously, the distribution of these products is different, depending on the reaction conditions and conversion. It should also be no noted that deprotonation in MA1 takes place with a different equilibrium constant than that of substrate (first addition pK_a (MeAcOAc)= 12, second addition pK_a (MA1)= 13).

As Table 1 shows, using NaOH as base the reaction took place with high conversions, but with a relatively low selectivity to the MA1 (Entry 1). Contrarily, the presence of $\overline{Au}$/fl-G films as catalyst led to lower conversions, but with very high selectivity towards MA1 (Table 1, entry 2). A control performing the using NaOH as base in the presence of $\overline{Au}$/fl-G films afforded almost similar

results as for the reaction carried out in the sole presence of NaOH, indicating that under these conditions the role of $\overline{Au}$/fl-G could be negligible.

Changing the Michael donor from methyl acetoacetate (MeAcOAc) to ethyl acetoacetate (EtAcOAc) or isobutyl acetoacetate (IsoBuAcOAc), both the conversion of the Michael donor and the selectivity to MA1 highly increased (Table 1, entries 4 and 5). This behavior indicates a higher reactivity of both EtAcOAc and IsoBuAcOAc, but shows the scope of $\overline{Au}$/fl-G films as Michael catalyst. Note that for EtAcOAc and IsoBuAcOAc formation of the second Michael addition product (MA2, Scheme 1) was notable, although lower than the selectivity reached for MeAcOAc using NaOH.

For the case of the cyclic esters (Scheme 2 and Table 2), only monoaddition to form MA1 ius possible, since MA1 does not possess an additional active hydrogen able to promote a subsequent Michael addition. Interestingly enough no 1,2 addition took place, the reaction following a 1,4 addition.

As expected in view of the acid/base properties of metal oxides, $\overline{Cu_2O}$/fl-G displays higher catalytic performance in Michael addition of both acetoacetates and cyclic esters donors with MVK acceptor than $\overline{Au}$/fl-G. However, at similar conversions $\overline{Au}$/fl-G exhibits somewhat higher selectivity to MA1 product than those measured for $\overline{Cu_2O}$/fl-G. This behavior can be related to the different acid/basic properties of $\overline{Au}$/fl-G in comparison to those of $\overline{Cu_2O}$/fl-G.

Michael addition is a reaction typically catalyzed by base catalysts. To evaluate the basicity of the investigated catalysts CO_2-TPD experiments were performed. Table 3 compiles these measurements for $\overline{Cu_2O}$/fl-G and $\overline{Au}$/fl-G films. Although the values are similar for both films, indicating the basicity of both films are similar, the data of CO_2 desorption were slightly higher for $\overline{Au}$/fl-G and, therefore, should be the reason of the somewhat different catalytic performance of the two films in the Michael addition. The CO_2 desorption data are somehow in line with the XPS results showing for Au, mainly the oxidation state (0) and for copper (I) and (II), what would imply some Lewis acidity on the positive metal ion.

Table 3. Amount of CO_2 desorbed as a function of the desorption temperature measured in the CO_2-TPD¡ for the investigated $\overline{Cu_2O}$/fl-G and $\overline{Au}$/fl-G catalysts

Catalyst	Desorption temperature °C	Quantity μmol/g	Total μmol/g
$\overline{Cu_2O}$/fl-G	134	10	25
	215	15	
$\overline{Au}$/fl-G	134	13	32
	215	19	

3. Conclusions

It has been shown that films of oriented 2.0.0 Cu_2O and 1.1.1 Au nanoplatelets grafted onto few-layers graphene are catalysts exhibiting activity in a series of reactions as Ullmann-type homocoupling, C–N cross-coupling and Michael addition, with TON values orders of magnitude higher than those of analogous Cu and Au catalysts adsorbed on graphene. In addition, films of these Cu2O and Au grafted on graphene also exhibit a remarkable catalytic activity to promote in the absence of any extrinsic base the Michael addition of acyclic and cyclic active methylene and methine compounds to $\alpha,\beta-$conjugated ketone. The catalytic activity has been rationalized based on the XPS measurements and CO_2-TPD analyses, the latter showing that these films exhibit some basicity.

4. Experimental

4.1. Catalyst preparation and characterization

The films used as catalysts in this study were prepared in accordance to previously reported procedures [Primo, A., Esteve, I., Blandez, J. f., Dhakshinamoorthy, A., Alvaro, M., Candu, N., Coman, S., Parvulescu, V., Garcia, H. *Nature Commun*., (2015), *Article number: 8561*; Primo A., Esteve-Adell I., Candu N., Coman S., Parvulescu V., Garcia H. (2016): *Angew. Chem.-Int. Ed.,* 55 (2), 607-612]. Briefly, the pristine fl-G used to adsorb Au or Cu_2O NPs as control catalysts was obtained by pyrolysis of sodium alginate extracted from brown algae (Sigma) under argon atmosphere (1 ml×min^{-1}), and using the following oven program: annealing at 200 °C for 2 h and, then, heating at 10 °Cmin^{-1} up to 900 °C for 6 h. The resulting graphitic powder was sonicated at 700 W for 1 h in water and the residue removed by centrifugation to obtain fl-G dispersed in water.

4.1.1. Adsorption of NPs (0.1wt%Au, 1.0 and 0.1 wt% Cu₂O) onto fl-G carrier

A mixture of 100 mg fl-G material, obtained as previously indicated, in 40 mL ethylene glycol was sonicated at 700 W for 1 h. Then, 0.2 mg of $HAuCl_4$ was added to the mixture under continuous stirring at 120 °C for 24 h. The obtained Au/fl-G was finally separated by filtration and washed exhaustively with water and acetone. The remained water was then removed in a vacuum desiccator at 110°C.

The same procedure was applied for the Cu NPs deposition, with the specification that for the synthesis of 1.0 or 0.1 wt% Cu_2O/fl-G, 10.6 or 1.06 mg $CuCl_2$ was used for 100 mg fl-G material.

4.1.2. Preparation of commercial Cu₂O/fl-G (0.1 wt%)

60 mg of fl-G was dispersed into 60 ml of ethanol using an ultrasound source (tip of 700 W) for 1 h. Then, 4.5 ml of commercial ethanolic suspension of Cu_2O (Aldrich, Ref: 678945, 1.5% (w/v)) was added and the mixture was stirred for 12 h to achieve deposition of the NPs onto fl-G.

4.1.3. The synthesis of oriented Au NPs and Cu NPs over few-layers graphene films ($\overline{Au}$/fl-G and $\overline{Cu}$/fl-G)

In 25 ml of a slightly acidified aqueous solution by addition of acetic acid (0.23 g), low molecular weight chitosan (0.5 g, Aldrich) was dissolved. Then viscous gel was then filtered through a syringe of 0.45 mm pore diameter to remove insoluble impurities present in the commercial chitosan. The chitosan films were supported on a quartz plate (2×2 cm^2) by casting 500 μL of filtered solution at 4000 rpm for 1 min. The obtained plates were immersed in a $HAuCl_4$ solution for 1 min, then pyrolysed under argon atmosphere (1 ml×min^{-1} flow) using the following program: heating rate at 5 °Cmin^{-1} up to 900 °C for 2 h.

For the synthesis of $\overline{Cu}$/fl-G films, the same procedure was applied with the specification that the 0.5 g chitosan were dissolved in a copper(II) nitrate aqueous solution (18 mg of $Cu(NO_3)_2 \times 2\frac{1}{2}$ H_2O in 25 ml of water) with a small quantity of acetic acid (0.23 g). The next preparation steps were similar to those used for the synthesis of the oriented $\overline{Au}$/fl-G sample.

Irrespective of the metal NPs nature or of the applied procedure, the metal content (ie, Au or Cu) on the films was determined by inductively coupled plasma optical emission spectrometry (ICP-OES) by measuring the metal content in the resulted solution from immersing the quartz plate into *aqua regia* (HNO_3/HCl 1:3) at room temperature for 3 h.

The prepared catalysts were exhaustively characterized using different techniques as powder X-ray diffraction (XRD), Raman spectroscopy, X-ray photoelectron spectroscopy (XPS) and transmission electron microscopy (TEM). All used techniques are described in detail in Refs. [Primo, A., Esteve, I., Blandez, J. f., Dhakshinamoorthy, A., Alvaro, M., Candu, N., Coman, S., Parvulescu, V., Garcia, H. *Nature Commun.*, (2015), *Article number: 8561*; Primo A., Esteve-Adell I., Candu N., Coman S., Parvulescu V., Garcia H. (2016): *Angew. Chem.-Int. Ed.,* 55 (2), 607-612]. CO_2-TPD measurements were carried out using an AutoChem II 2920 instrument. The samples (3-5 mg), placed in a U-shaped quartz reactor with an inner diameter of 0.5 cm, were pretreated with He (Purity 5.0, from Linde) at 120 ℃ for 1 h, and then exposed to a flow of CO_2 (from SIAD) for 1 h. After that, the sample was purged with a flow of He (50 mL min^{-1}) for 20 min at 25 ℃ to remove weakly adsorbed CO_2. TPD was then started, with a heating rate of 10 ℃ min^{-1} till 850 ℃. The desorbed products were analyzed with a TC detector. The CO_2 desorbed, expressed as μmoles of CO_2 per gram of catalyst, was determined using a calibration curve.

4.2. Catalytic tests

All reagents were purchased from Sigma-Aldrich and used as received without any further purification.

4.2.1 C–N coupling procedure

To a solution of bromobenzene (1.2 mmol) and aniline (1 mmol) in 4 mL of 1,4-dioxane, potassium tert-butoxide ($KOCH_3$, 2.1 mmol) and catalyst (ie, two flat pieces of 1×1 cm^2 films of $\overline{Cu_2}O$/fl-G on quartz (0.24 mg of Cu total), 10 mg of unoriented Cu_2O/fl-G powder containing 1.0 or 0.1 wt% Cu, 1 × 1 cm^2 plate of $\overline{Au}$/fl-G film or 10 mg of Au/fl-G powder containing 0.1 wt% Au loading) was added. The resulting mixture was stirred in an autoclave for 24 h at 200 °C.

4.2.2. Ullmann-like homocoupling procedure.

To a solution of iodobenzene, (2.0 mmol) in 4 ml of 1,4-dioxane, $KOCH_3$ (2 mmol) and catalyst (ie, two flat pieces of 1×1 cm^2 of $\overline{Cu_2}O$/fl-G on quartz (0.24 mg of Cu total), 10 mg of unoriented Cu_2O/fl-G powder containing 1.0 or 0.1 wt% Cu, one piece of 1 × 1 cm^2 plate of $\overline{Au}$/fl-G film or 10 mg of Au/fl-G powder containing 0.1 wt% Au loading) were added. The resulting mixture was stirred in an autoclave for 24 h at 160 °C.

4.2.3. Michael addition procedure

To a solution of β-ketoesters as Michael donor (1 mmol of methyl acetoacetate, ethyl acetoacetate; isobutyl acetoacetate, ethyl 2-oxocyclohexanecarboxylate or ethyl 2-oxocyclopentanecarboxylate) in 8 ml of solvent (deionized H_2O) was added MVK as Michael acceptor (1.5 mmol, 0.105 g), base (0.12 mmol, NaOH) if required and one piece of 1 × 1 cm^2 plate of $\overline{Au}$/fl-G film catalyst. The resulting mixture was left stirring at room temperature for 18 h. The reaction mixture was then filtered, extracted with ethyl ethanoate (3 x 10 mL) and the combined organic layer was dried over Na_2SO_4, filtered and concentrated.

4.2.4. Product analysis

Irrespective of reaction procedure, after reaction the catalyst was collected by filtration or was manually removed and the reaction products were analyzed and identified by GC-MS (THERMO Electron Corporation instrument), Trace GC Ultra and DSQ, TraceGOLD with a TG-5SilMS column (30 m × 0.25 mm × 0.25 mm).

Michael adducts using donors such as:

1. *Methyl acetoacetate*

MA1: Methyl 2-acetyl-5-oxohexanoate**: GC-MS, (m/z):186 (M$^+$, 2), 155 (12), 154 (12), 144 (100), 143 (18), 139 (25), 129 (15), 116 (40), 112 (56), 111 (57), 101 (21), 97 (17), 87 (64), 84 (64), 69 (17), 58 (20), 55 (29).

MA2: GC-MS, (m/z): 256 (M$^+$, 1), 238 (20), 196 (24), 186 (87), 182 (15), 181 (66), 179 (87), 167 (48), 165 (22), 164 (42), 154 (88), 153 (63), 143 (43), 139 (82), 137 (33), 136 (40), 129 (90), 125 (33), 123 (73), 116 (47), 111 (100), 109 (56), 97 (63), 95 (32), 93 (65), 91 (23), 85 (18), 84 (12), 79 (14), 71 (32), 55 (25).

2. *Ethyl acetoacetate*

MA1: Ethyl 2-acetyl-5-oxohexanoate: GC-MS, (m/z): 200 (M$^+$, 2), 158 (100), 139 (29), 130 (30), 112 (59), 111 (69), 101 (55), 84 (71), 73 (33), 55(17).

MA2: GC-MS, (m/z): 270 (M$^+$, 1), 252(18), 209 (24), 200 (100), 181 (98), 179 (88), 167 (52), 165 (32), 164 (30), 157 (39), 154 (55), 153(25), 143(76), 139 (91), 137 (29), 136 (31), 125 (29), 123 (60), 121 (54), 115 (16), 111 (90), 109 (52), 97 (43), 95 (27), 93 (51), 71 (16), 55 (14).

3. *Isobutyl acetoacetate*

MA1: Isobutyl 2-acetyl-5-oxohexanoate: GC-MS, (m/z): 228 (M$^+$, 2), 186 (56), 155 (39), 139 (36) 131 (43), 129 (25), 113 (36), 112 (99), 111 (75), 103 (27), 102 (27), 84 (100), 58 (32), 57 (48), 55 (17).

MA2: GC-MS, (m/z): 298 (M$^+$, 1), 280 (12), 238 (20), 228 (73), 209 (25), 185 (27), 182 (28), 181 (97), 179 (94), 171 (17), 167 (27), 165 (30), 164 (61), 163 (17), 158 (14), 154 (95), 153 (28), 140 (54), 139 (99), 137 (45), 136 (75), 125 (36), 123 (93), 122 (49), 121 (100), 115 (58), 11 (85), 109 (63), 103 (20), 97 (35), 93 (57), 71 (24), 57 (35), 55 (15).

4. *Ethyl 2-oxocyclopentanecarboxylate*

MA1: Ethyl 2-oxo-1-(3-oxobutyl)cyclopentanecarboxylate: GC-MS, (m/z): 226 (M$^+$, 2); 208 (14), 198 (50), 169 (11), 156 (38), 152 (45), 141 (18), 137 (47), 127 (15), 125 (100), 124 (20), 111 (70), 110 (66), 109 (39), 97 (37), 95 (27), 81 (16), 55 (20).

5. *Ethyl 2-oxocyclohexanecarboxylate*

MA1: Ethyl 2-oxo-1-(3-oxobutyl)cyclohexanecarboxylate: GC-MS, (m/z): 240 (M$^+$,1), 212 (10), 194 (32), 171 (13), 170 (100), 169 (12), 151 (48), 149 (29), 142 (43), 138 (23), 136 (26), 125 (45), 123 (61), 111(21), 109 (37), 95 (34), 81 (39), 67 (15), 55 (21).

References